Research Article Vol. 30, No. 9 / 25 Apr 2022 / Optics Express 15073
Optics EXPRESS

Numerical study of absorption-enhanced parametric amplification

GINTARAS VALIULIS* AND ARŪNAS VARANAVIČIUS

Laser Research Center, Vilnius University, Saulėtekio10, 10223 Vilnius, Lithuania
*gintaras.valiulis@ff.vu.lt

Abstract: Usually the absorption of interacting waves is detrimental to the parametric amplification process. We show that even in the case of large idler wave absorption it is possible to get highly efficient signal amplification as well as amplifier bandwidth enhancement due to back-conversion suppression. We numerically investigated the influence of the idler wave linear losses arising in the case of parametric amplification in 515 nm pumped BBO crystal tuned to signal amplification at 610 nm. The possibility to achieve ~75% pump-to-signal energy conversion and amplification bandwidth of ~900 cm^{-1} using collinear amplification scheme is demonstrated.

1. Introduction

The optical parametric amplification (OPA) process is an effective method to generate wavelength tunable light pulses and can provide large amplification bandwidths needed for ultrashort light pulses formation [1]. The waves amplified by pump wave in optical parametric amplifier are called signal and idler, and both of them can be useful for applications. The efficiency of parametric pump energy conversion to amplified signal fundamentally is limited by backconversion effect and typically is around ~20%. Moreover, the backconversion also introduces significant spatiotemporal distortions of output radiation [2]. Usually, it is common opinion that the absorption of the signal or idler waves is a detrimental phenomenon, reducing the efficiency of the OPA. However, there have been published several papers showing that losses introduced to idler wave may lead to improvement of OPA characteristics. A couple decades ago, Lowenthal studied the influence of the idler wave absorption to the parametric amplification process in continuous wave regime. This study showed that some idler absorption can raise the signal output power [3]. In parametric oscillators the losses introduced for the idler wave leads to suppression of pump back conversion and improvement of both signal conversion efficiency as well as signal beam quality can be obtained [4,5]. The numerical simulation of multi-pass OPA in conditions of undepleted pump and strong idler absorption revealed also the possibilities for a significant OPA bandwidth broadening [6,7]. The energy conversion enhancement due to pump reconversion suppression has been demonstrated experimentally in non-collinear chirped pulse parametric amplification system employing type I phase matching Sm^3-doped yttrium calcium oxyborate crystal that possess strong absorption band in spectral range of idler wavelength [8]. The setup is robust against phase mismatch and supports 90 fs pulse amplification at 800 nm. Even broader amplification bandwidth and back conversion circumvention can be obtained using special idler-separated non-collinear amplification design based on periodically poled MgO: $LiNbO_3$ [9].

In this work we examine analytically the parametric amplification in presence of idler absorption and present the results of numerical simulation of OPA operated in strong nonlinear regime. In this study we explore the 610 nm signal amplification in BBO crystals pumped by 515 nm wavelength pulses fulfilling the condition of strong losses for idler. The modeling was performed for different pump pulse durations and pump beam profiles using new data available due to recent

#456019 https://doi.org/10.1364/OE.456019
Journal © 2022 Received 10 Feb 2022; revised 28 Mar 2022; accepted 30 Mar 2022; published 20 Apr 2022

Optics EXPRESS

measurements of the BBO crystal transparency and dispersion properties in infrared region [10,11].

2. Theory

In order to explore analytically the influence of absorption to optical parametric amplification process, we will start with the set of equations describing the OPA:

$$\begin{aligned}
&\frac{\partial A_1}{\partial z} + \nu_{13}\frac{\partial A_1}{\partial t} - \frac{i}{2}g_1\frac{\partial^2 A_1}{\partial t^2} - h_1\frac{\partial^3 A_1}{\partial t^3} + \alpha_1 A_1 = -i\sigma_1 A_2^* A_3 \exp(-i\Delta k\, z),\\
&\frac{\partial A_2}{\partial z} + \nu_{23}\frac{\partial A_2}{\partial t} - \frac{i}{2}g_2\frac{\partial^2 A_2}{\partial t^2} - h_2\frac{\partial^3 A_2}{\partial t^3} + \alpha_2 A_2 = -i\sigma_2 A_1^* A_3 \exp(-i\Delta k\, z),\\
&\frac{\partial A_3}{\partial z} - \frac{i}{2}g_3\frac{\partial^2 A_3}{\partial t^2} - h_3\frac{\partial^3 A_3}{\partial t^3} + \alpha_3 A_3 = -i\sigma_3 A_1 A_2 \exp(+i\Delta k\, z).
\end{aligned} \tag{1}$$

where $A_j(t,z)$ is the wave complex amplitude, t is the retarded time (corresponding to the coordinate frame moving with the pump wave), z is longitudinal coordinate. The j =1, 2, 3 stand for signal, idler and pump waves, respectively. $\nu_{j3} = u_j^{-1} - u_3^{-1}$ is the group velocity mismatch (GVM) coefficients, u_j is the group velocity of wave j calculated at carrier frequency ω_{j0}, and for the carrier frequencies we have constraint $\omega_{10} + \omega_{20} = \omega_{30}$, typical for three-wave interaction process. Parameters $g_j = d^2k/d\omega^2|_{\omega_{j0}}$ are the group velocity dispersion (GVD) coefficients, $h_j = {}^1\!/_6 d^3k/d\omega^3\Big|_{\omega_{j0}}$ are the third order dispersion coefficients. k_j is the absolute value of the wave j axial wave-vector. σ_j is the nonlinear coupling coefficient. Δk is the phase mismatch. Note, that the material dispersion is accounted till the third order. The linear absorption is accounted by adding the $\alpha_j A_j$ terms and assumed being frequency independent over all pulse spectral frequency range. In case of frequency dependent absorption it can be accounted via inclusion of the integral terms

$\int_0^\infty \bar{\alpha}_j(\tau)A_j(t-\tau)d\tau$, (where $\bar{\alpha}_j(t) = \frac{1}{2\pi}\int_{-\infty}^{+\infty}\alpha_j(\omega)\exp(i\omega t)d\omega$) to the left side of equations (1), instead of the $\alpha_j A_j$. In case of plane, monochromatic and undepleted pump wave ($|A_1|,\ |A_2| \ll |A_3|, A_3 = const. = A_{30}$) instead of Eq. (1) we have system of two linear equations:

$$\begin{aligned}
&\frac{\partial A_1}{\partial z} + \nu_{13}\frac{\partial A_1}{\partial t} - \frac{i}{2}g_1\frac{\partial^2 A_1}{\partial t^2} - h_1\frac{\partial^3 A_1}{\partial t^3} + \alpha_1 A_1 = -i\sigma_1 A_2^* A_{30} \exp(-i\Delta k\, z),\\
&\frac{\partial A_2}{\partial z} + \nu_{23}\frac{\partial A_2}{\partial t} - \frac{i}{2}g_2\frac{\partial^2 A_2}{\partial t^2} - h_2\frac{\partial^3 A_2}{\partial t^3} + \alpha_2 A_2 = -i\sigma_2 A_1^* A_{30} \exp(-i\Delta k\, z).
\end{aligned} \tag{2}$$

The solution of the set of the Eq. (2) can be found in spectral domain using Fourier transform:

$$A_j(t,z) = \frac{1}{2\pi}\int_{-\infty}^{\infty} S_j(\omega,z)\exp(i\omega t)d\omega \tag{3}$$

By substituting Eq. (3) into Eq. (2) we obtain the set of the ordinary differential equations in spectral domain. The exact analytic solution of these equations reads:

$$S_1(\omega,z) = [S_{10}(\omega)\cosh(\Gamma(\omega)z) - iR_{10}(\omega)\sinh(\Gamma(\omega)z)]\exp[-iD(\omega)z], \tag{4}$$

$$S_2^*(-\omega,z) = [S_{20}^*(-\omega)\cosh(\Gamma(\omega)z) + iR_{20}(\omega)\sinh(\Gamma(\omega)z)]\exp[-iD(\omega)z], \tag{5}$$

$$R_{10}(\omega) = \frac{K(\omega)S_{10}(\omega) + \sigma_1 a_3 S_{20}^*(-\omega)}{\Gamma(\omega)}, \tag{6}$$

$$R_{20}(\omega) = \frac{K(\omega)S_{20}^*(-\omega) + \sigma_2 a_3 S_{10}(\omega)}{\Gamma(\omega)}, \tag{7}$$

$$\Gamma(\omega) = \sqrt{\Gamma_0^2 - K(\omega)^2}, \tag{8}$$

Optics EXPRESS

$$D(\omega) = D_0(\omega) - \frac{i}{2}[\alpha_2(-\omega) + \alpha_1(\omega)], \tag{9}$$

$$K(\omega) = K_0(\omega) + \frac{i}{2}[\alpha_2(-\omega) - \alpha_1(\omega)], \tag{10}$$

$$D_0(\omega) = \frac{1}{2}\left[(\nu_{13} + \nu_{23})\omega + \frac{1}{2}(g_1 - g_2)\omega^2 + (h_1 + h_2)\omega^3 + \Delta k\right], \tag{11}$$

$$K_0(\omega) = \frac{1}{2}\left[\nu_{12}\omega + \frac{1}{2}(g_1 + g_2)\omega^2 + (h_1 - h_2)\omega^3 - \Delta k\right], \tag{12}$$

where $\Gamma_0 = \sqrt{\sigma_1\sigma_2}A_{30}$ is the parametric gain increment for the case of plane and monochromatic waves.

For future analysis we assume perfect phase-matching $\Delta k = 0$, no incident idler $S_{20}(\omega) = S_2(\omega, z = 0) = 0$. Also we assume large gain parameter $\Gamma_0 z \gg 1$.

We define the frequency ω as detuning from carrier, thus for signal wave frequencies we have $\omega_1 = \omega_{10} + \omega$, and for idler $\omega_2 = \omega_{20} - \omega$, respectively. Note, that in solution (Eqs. (9), (10)) the absorption parameters are frequency dependent, for generality, but since we are presenting solutions in frequency domain, it does not make any difference to the form of solution, thus further we denote $\alpha_1 = \alpha_1(\omega)$, $\alpha_2 = \alpha_2(-\omega)$, just keeping in mind that the absorption coefficients could be dispersive.

Let's analyze several cases.

2.1. OPA without absorption

We assume $\alpha_1 = \alpha_2 = 0$, parameters $K(\omega), D(\omega)$ becomes real $K(\omega)$=$K_0(\omega)$, $D(\omega) = D_0(\omega)$, and, in the case of large gain when $\Gamma_0 z \gg 1$ (,) the approximate solution is:

$$\begin{gathered} S_1(\omega, z) \approx \tfrac{1}{2}S_{10}(\omega)\exp(\Gamma(\omega)z)\exp(-iD_0(\omega)z), \\ S_2^*(-\omega, z) \approx i\sqrt{\tfrac{\sigma_2}{\sigma_1}}S_1(\omega, z). \end{gathered} \tag{13}$$

From analysis of the Eqs. (8-13) the following conclusions can be done. The parameter $D_0(\omega)$, i.e. so-called nonlinear dispersion, describes the evolution of the spectral phase during propagation, whereas the parameter $\Gamma(\omega)$ defines the gain of the spectral components. The gain bandwidth of the parametric amplifier becomes infinite if the gain for all the spectral components is uniform: $\Gamma(\omega) = const$. This condition requires $K(\omega) = 0$. Such condition could be satisfied in OPA with angularly dispersed waves (X pulses, for example) [12] due to extra degree of freedom *i.e.* the K parameter becomes dependent on spatial frequency $k_\perp$ (transverse wave-vector), and condition $K(\omega, k_\perp) = 0$ just means the phase-matching of different wavelengths at slightly different angles. It is sometimes called the achromatic phase matching [13].

In case of large beams and no pulse front tilting the fulfilment of condition $K(\omega) = 0$ becomes impossible due to material dispersion and narrow angular spectrum. It can be approximately fulfilled just in vicinity the carrier frequency. However, if the spectral width of the gain $\Gamma(\omega)$ curve is much larger than the bandwidth of the amplified pulse all spectral components of the pulse have nearly uniform amplification. Considering just the first dispersion approximation

Optics EXPRESS

($K_0(\omega) = 1/2(\nu_{12}\omega)$) we obtain

$$S_1(\omega, z) \approx \frac{1}{2} S_{10}(\omega) \exp(\Gamma_0 z) \exp\left(-z \frac{\nu_{12}^2 \omega^2}{8\Gamma_0^2}\right) \exp(-iD_0(\omega)z). \tag{14}$$

From the Eq. (14), the well-known expression for the OPA amplification bandwidth can be derived:

$$\Delta\omega_{opa} = 4\sqrt{\frac{\ln 2 \Gamma_0}{\nu_{12}^2 z}}. \tag{15}$$

Note that dispersion characteristics of interacting pulses is modified by nonlinearity and is accounted via parameter $D_0(\omega)$. The signal and idler waves propagates with the same group velocity (defined by averaged group mismatch parameter $(\nu_{13} + \nu_{23})/2$) and can have the suppressed GVD (if the both GVD parameters g_1 and g_2 are of the same sign).

2.2. OPA with absorption of both signal and idler waves

Let's assume $\alpha_1 = \alpha_2 = \alpha \neq 0$. Such a situation could take place near degeneracy when $\omega_{10} \approx \omega_{20}$ and both signal and idler waves are in infrared wavelength region.

For such conditions $K(\omega)$ remains real $K(\omega) = K_0(\omega)$, but $D(\omega)$ becomes complex $D(\omega) = D_0(\omega) - i\alpha$. Thus, instead of Eq. (14) we obtain (for the 1-st approximation of dispersion):

$$S_1(\omega, z) \approx \frac{1}{2} S_{10}(\omega) \exp([\Gamma_0 - \alpha]z) \exp\left(-z \frac{\nu_{12}^2 \omega^2}{8\Gamma_0^2}\right) \exp(-iD_0(\omega)z). \tag{16}$$

As can be seen from Eq. (16) the terms responsible for bandwidth and nonlinear dispersion remains unchanged (as in lossless medium) but the gain drops and at $\alpha = \Gamma_0$ vanishes.

2.3. OPA with absorption just of the idler

Let's analyze situation when OPA operates far from the degeneracy and the idler falls into the wavelengths range of high absorption. Thus, we assume $\alpha_1 = 0$, $\alpha_2 \neq 0$. Also we suppose $\Delta k = 0$, $S_{20}(\omega) = 0$, $\Gamma_0 z \gg 1$, and $\Gamma_0 z \gg K_0(\omega)$. For such case both parameters $K(\omega)$, $D(\omega)$ are complex $K(\omega) = K_0(\omega) + i\alpha_2/2$, $D(\omega) = D_0(\omega) - i\alpha_2/2$, and from Eqs. (4-12) follows:

$$S_1(\omega, z) \approx \frac{1}{2} S_{10}(\omega) \exp\{G(\omega)z\} \exp(-iD_0(\omega)z), \tag{17}$$

where

$$G(\omega) = \sqrt{{\Gamma_0}^2 - \left[K_0(\omega) + \frac{i}{2}\alpha_2\right]^2} - \frac{1}{2}\alpha_2 . \tag{18}$$

In case when the idler wave absorption is dominant over material dispersion ($\alpha_2 \gg K_0(\omega)$) we have

$$G(\omega) \approx \sqrt{{\Gamma_0}^2 + \frac{1}{4}\alpha_2^2} - \frac{1}{2}\alpha_2 \tag{19}$$

Thus, even for very large idler absorption the gain of the spectral components is always positive and its frequency dependence is defined only by absorption dispersion $\alpha_2 = \alpha_2(\omega)$. That could lead to broadening of the OPA amplification bandwidth. Moreover, even in the case when $\alpha_2 \gg \Gamma_0 \gg K_0(\omega)$ the gain is still exponential, just the argument of the exponent is reduced by factor $\Gamma_0/\alpha_2(\omega)$:

$$S_1(\omega, z) \sim \exp(-iD_0(\omega)z) \exp\left\{\Gamma_0 z \frac{\Gamma_0}{\alpha_2(\omega)}\right\}. \tag{20}$$

The exponential gain, despite large absorption of one wave could be explained, keeping in mind the quantum nature of the OPA process: pump photons of the frequency ω_3 are splitting into

Optics EXPRESS

signal and idler photons with the frequencies ω_1 and ω_2, accordingly to the energy conservation rule $\omega_3 = \omega_1 + \omega_2$. Even if the idler wave is absorbed the generated signal photons are sustaining the growth of the signal wave. The influence of idler absorption on the OPA bandwidth under conditions of undepleted pump was already studied in our previous papers [6,7].

However, the parametric amplification in the regime of substantial pump depletion that is usually present in parametric power booster amplifiers can significantly impact the amplification dynamics due to pump regeneration processes. Since pump back conversion can be suppressed by introducing loses for one of the amplified waves we have performed numerical OPA simulation in the nonlinear crystal tuned to signal amplification wavelength at which the idler is strongly absorbed.

3. OPA in regime of strongly depleted pump and idler absorption

The numerical experiments were conducted for OPA based on BBO nonlinear crystal. As it was mentioned above the dispersive properties and absorption coefficients of the BBO crystal were taken from [10,11]. The study was done for 3 different pulse duration regimes: 10 ps, 1 ps and 100 fs. In all cases pump wavelength was $\lambda_3 = 515$ nm ("e" – polarization), signal $\lambda_1 = 610$ nm ("o" – polarization) and idler $\lambda_2 = 3.3\,\mu$m ("e" – polarization). Absorption is significant for infrared idler wave. The absorption coefficient, according [10,11] at 3.3 μm is $\alpha_2 = 1.25\,\mathrm{mm}^{-1}$. In numeric experiment instead of α parameter we used the absorption length, defined as $L_{\alpha 2} = (2\alpha_2)^{-1}$. In our case $L_{\alpha 2} = 0.4$ mm that corresponds to pulse intensity dropping by factor "e" after the linear propagation of 0.4 mm in the crystal. The pump was transform-limited Gaussian pulse and transform-limited or positively/negatively chirped Gaussian pulses with complex amplitude $A_j = a_{j0}\exp(-t^2/\tau_{j0}^2(1 + i\gamma))$, where γ defines pulse chirp, is used as an OPA seed. Note, that most of calculations were performed for the plain wave model solving numerically the set of Eq. (1). In order to reveal realistic OPA parameters we also performed 3D numerical simulations using pulsed Gaussian and hyper-Gaussian beams. The results of these simulations are presented at the end of this section.

3.1. 10 ps regime

The initial OPA parameters are: pump pulse intensity $I_3 = 10$ GW/cm^2, pump pulse duration $\tau_3 = 10$ ps, signal pulse intensity at input $I_1 = 0.01$ GW/cm^2, signal pulse duration $\tau_2 = 20$ ps. Calculations were performed for the three different chirp values: $\gamma = 0, \pm 1000$. The incident chirped signal pulse spectrum width for the cases of $\gamma = \pm 1000$ corresponds to the 20 fs transform-limited pulse duration.

The dependences of the amplified signal pulse intensity, duration, conversion efficiency and bandwidth on propagation distance are presented in Fig. 1. Black lines with circles represents the case of transform-limited signal ($\gamma = 0$), blue with triangles ($\gamma = -1000$) and red lines with squares ($\gamma = 1000$). In order to highlight the influence of idler absorption on the dynamics of amplification we added to the graphs the variation of output parameters for the case of artificially switched-off idler absorption. In fact these dependencies quite similar to the results of numerical simulations performed for the case of 650 nm pulse amplification. At this signal wavelength the idler is at ~2600 nm and experiences rather small losses due to linear absorption. As one can see the absorption of idler wave determines completely different amplification regime respect to lossless case. The conversion efficiency in case of no idler absorption oscillates with propagation distance corresponding to phases of pump reconversion. The oscillations in the graphs depicting changes in pulse and spectrum envelope widths at half maximum represents complicated dynamics of amplified pulse splitting and fragmentation. When idler absorption is accounted the energy transfer from pump to signal continuously rises with parametric interaction distance till nearly total pump depletion is reached and the pump conversion to the signal approaches the value of ~80% (theoretical limit is 84%).

Optics EXPRESS

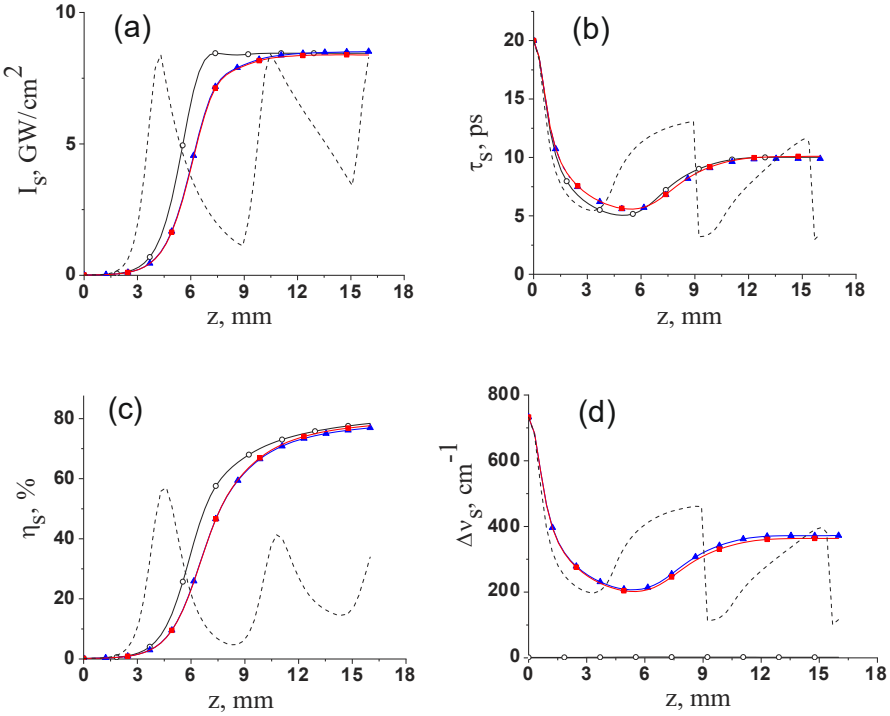

Fig. 1. Variation of amplified signal pulse intensity (a), duration (b), pump-to-signal conversion efficiency (c) and amplified pulse bandwidth (d) with propagation distance z. Pump pulse duration 10 ps. Input signal pulse cases are: no chirp (black lines with circles), negative chirp (blue lines with triangles), positive chirp (red lines with squares). Dash lines represent lossless case. See text for more details.

Figure 1 shows that for the 10 ps duration case the amplification dynamics is not sensitive to the sign of chirp. Also in all three cases of the chirp ($\gamma = 0\,,\ \pm 1000$) pulse profiles are nearly similar. Pulse profiles after 12 mm propagation in BBO are depicted in Fig. 2, signal (black solid), idler (red dash-dot) and pump blue dash). Figure 2(a) presents the amplified signal profile for the case of initial chirp $\gamma = -1000$. The 73% of pump energy is converted to signal. Since our OPA sustains quite large bandwidth ($\Delta\nu \approx 370$ cm^{-1}, Fig. 1(d)) the initially chirped and amplified signal pulse was numerically compressed from 9.8 ps down to 62 fs (inset, Fig. 2(a)). The intensity correspondingly is raising from 8.4 GW/cm^2 up to ~1.2 TW/cm^2 However, in the lossless case (Fig. 2(b)) the pulse profiles are much more complicated and energy conversion to signal is just 19%.

3.2. 1 ps regime

In this case the initial OPA parameters are: pump pulse intensity $I_3 = 50$ GW/cm^2, pump pulse duration $\tau_3 = 1$ ps, signal pulse intensity at input $I_1 = 0.01$ GW/cm^2, signal pulse duration $\tau_2 = 2$ ps. Calculations were performed for the three different chirp values: $\gamma = 0, \pm 200$ The incident chirped signal pulse spectrum width ($\gamma = \pm 200$) corresponds to the 10 fs transform-limited pulse duration.

The parameters of amplified signal are depicted in Fig. 3. Black lines with circles represents the case of transform-limited signal ($\gamma = 0$), blue with triangles ($\gamma = -200$) and red lines with squares ($\gamma = 200$). Also the dependences for the case of artificially switched-off absorption is

Optics EXPRESS

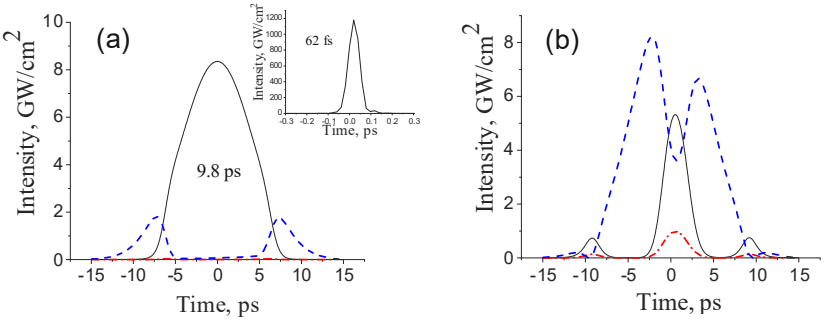

Fig. 2. The profiles of signal (black solid), idler (red dash-dot), pump (blue dash) pulses calculated for propagation distance of 12 mm. (a) the profiles in presence of idler absorption, (b) profiles when idler absorption is not accounted. Inset in (a) shows the amplified and compressed pulse envelope. Pump duration is 10 ps.

added to the plots (dash lines). The profiles of amplified pulses in 8 mm BBO are shown in Fig. 4. As in the case of 10 ps pump the absorption of idler wave quenches the back-conversion.

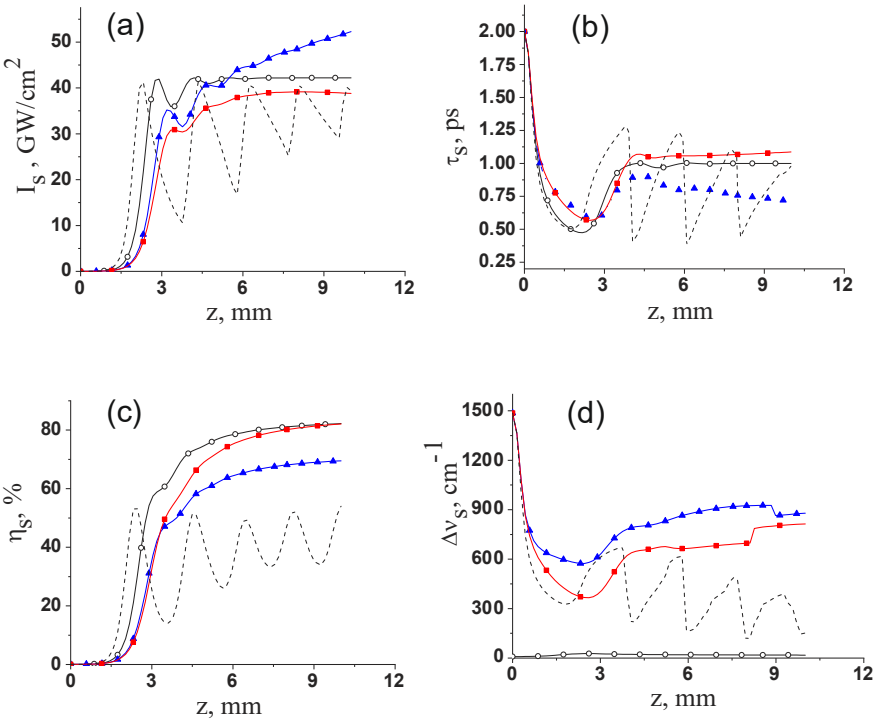

Fig. 3. Variation of amplified signal pulse intensity (a), duration (b), pump-to-signal conversion efficiency (c) and amplified pulse bandwidth (d) with propagation distance z. Input signal pulse cases are: no chirp (black lines with circles), negative chirp (blue lines with triangles), positive chirp (red lines with squares). Dash lines represent lossless case. Pump pulse duration 1 ps.

As can be seen from Fig. 3 for $\gamma = 0$ and $\gamma = +200$ amplification becomes saturated, with the conversion to the signal efficiency ~81%, with the signal duration 1ps and 1.1ps, respectively

Optics EXPRESS

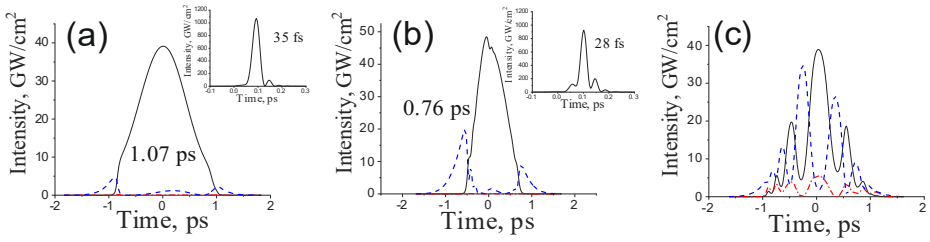

Fig. 4. The profiles of signal (black solid), idler (red dash-dot), pump (blue dash) pulses calculated for propagation distance of 8 mm. (a) profiles for phase modulated input signal with $\gamma = 200$, (b) profiles for phase modulated input signal with $\gamma = -200$, (c) profiles when idler absorption is not accounted. Insets show the amplified and compressed pulse envelopes. Pump duration is 1 ps.

(Fig. 3(a), Fig. 4(a)). For the case $\gamma = -200$ efficiency is less (~70%) because of signal pulse compression down to 0.76 ps. OPA has a bandwidth of $\Delta\nu \approx 900$ cm^{-1} (see Fig. 2(d)), thus 1 ps amplified pulses the pulse with $\gamma = +200$ can be compressed down to 35 fs (inset, Fig. 4(a)).

For the negative chirp ($\gamma = -200$) case the compressed pulse duration is 28 fs (inset, Fig. 4(b)). In the lossless regime (switched-off absorption) the multiple reconversion cycles (Fig. 3, dash lines)), complicated pulse shape (Fig. 4(c)) and much lower conversion efficiency (Fig. 3(c)) are observed.

3.3. 100 fs regime

The femtosecond pulse regime was studied for the following initial parameters: pump pulse intensity $I_3 = 60$ GW/cm^2, pump pulse duration $\tau_3 = 100$ fs, signal pulse intensity at input $I_1 = 0.01$ GW/cm^2, signal pulse duration $\tau_2 = 200$ fs. Calculations were performed for the three different chirp values:$\gamma = 0, -20, +20$. The incident chirped signal pulse spectrum width with $|\gamma| = 20$ corresponds to the 10 fs transform-limited pulse duration.

Output characteristics are presented in Fig. 5. Black lines with circles represents the case of transform-limited signal ($\gamma = 0$), blue with triangles ($\gamma = -20$) and red lines with squares ($\gamma = 20$). Amplification in conditions of no idler absorption is illustrated by dashed lines. The profiles of amplified pulses are shown in Fig. 6. As in the previous cases the absorption of idler wave quenches the back-conversion and for all chirp values the conversion efficiency raises monotonically to saturation reaching ~80-82% (Fig. 5(c)). The signal durations are 109 fs ($\gamma = 0$, Fig. 6(a)), 121 fs ($\gamma = 20$, Fig. 6(b)) and 154 fs ($\gamma = -20$, Fig. 6(c)). A new peculiarity caused by nonlinear dispersion manifestation arises in femtosecond regime. According to Eq. (11) the signal wave effective group velocity dispersion coefficient is $g_1^{eff} = \frac{1}{2}(g_1 - g_2)$, but the idler wave ($\lambda_2 = 3.3$ μm) is in anomalous GVD region where $g_2 < 0$ with the magnitude ~11 times larger than one for the signal ($|g_2| \approx 11 g_1$), thus we have $g_1^{eff} \approx \frac{1}{2}|g_2|$. It seems, that 100 fs pulse is short enough to feel GVD in just 2-5 mm of propagation in BBO. In order to describe GVD, instead of g_j we used GVD length defined as a distance when the transform-limited Gaussian pulse increase its duration τ by factor $\sqrt{2}$: $L_{gj} = \tau^2/(4 \ln 2 g_j)$. For 100 fs duration signal pulse GVD length in linear medium is $L_{g1} = 32$ mm, but taking into account nonlinear dispersion with the coefficient g_1^{eff}, we have $L_{g1} = 2.6$ mm. That explains the signal pulse duration dynamics (Fig. 5(b)). In transform-limited case ($\gamma = 0$, black line with circles) signal pulse decrease in duration (due to inhomogeneous amplification) down to 47 fs (at $z = 2$ mm) but later spreads dispersively up to 109 fs (at $z = 5$ mm, Fig. 6(a)), acquiring significant positive chirp. It might be compressed down to 30 fs (inset, Fig. 6(a)).

Optics EXPRESS

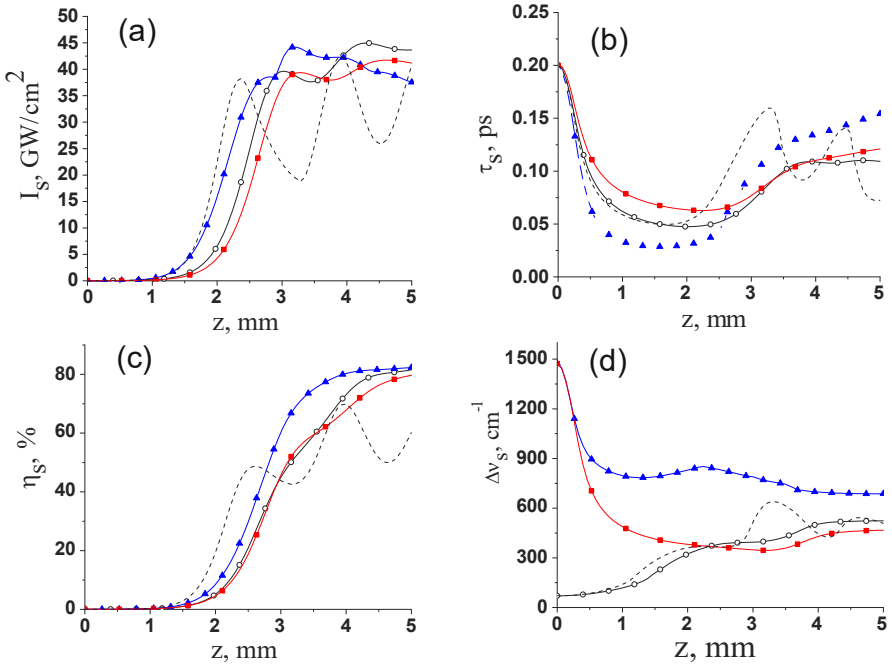

Fig. 5. Variation of amplified signal pulse intensity (a), duration (b), pump-to-signal conversion efficiency (c) and amplified pulse bandwidth (d) with propagation distance z. Input signal pulse cases are: no chirp (black lines with circles), negative chirp (blue lines with triangles), positive chirp (red lines with squares). Dash lines represent lossless case. Pump pulse duration 100 fs.

The initially positively chirped signal pulse ($\gamma = 20$, Fig. 5(b) red line with squares) due to positive chirp induced extra broadening minimizes its duration due to pump profile at $z = 2.2$ mm of propagation (63 fs). During further propagation the duration is dispersively growing till 121 fs (Fig. 5(b), Fig. 6(b)). The positive chirp acquired allows to compress signal pulse till 32 fs (inset Fig. 6(b). The negatively chirped ($\gamma = -20$) signal pulse demonstrates extra compression at 1.55 mm till 28 fs (Fig. 5(b), initially negatively chirped pulse becomes transform-limited and with the subsequent dispersive spreading till 154 fs accumulates positive chirp. (see also Fig. 6(c)). Such pulse could be compressed from 154 fs down to 26 fs (inset Fig. 6(c)).

The dashed lines in Figs. 1, 3, 5 depicts the lossless cases with the switched-off absorption. The oscillations represents the cycles of back-conversion. As one can see the depth of modulations become less when the pulse durations changing from picoseconds to femtoseconds. Also the profile of signal pulse (Fig. 6(d)) is much more regular respect to picosecond case (Fig. 5(c)). This represents the fact that huge GVD of idler virtually mimics the action of idler absorption. Large spreading of idler causes the energy flow outside the interaction region defined by pump pulse duration.

3.4. 3D modeling

The data presented in previous sections were obtained using 1D (plane wave) model. In order to evaluate the amplification parameters for pulsed beams we performed calculation for the 1 ps regime using 3D model and accounting both for pump and signal beam profiles. All initial OPA parameters were as in 3.2 section with the transform-limited signal pulse at the input. Two different spatial profiles for pump were used: hyper-Gaussian ($A_3 = a_{30}\exp(-r^6/d_{3H}^6)$) and

Optics EXPRESS

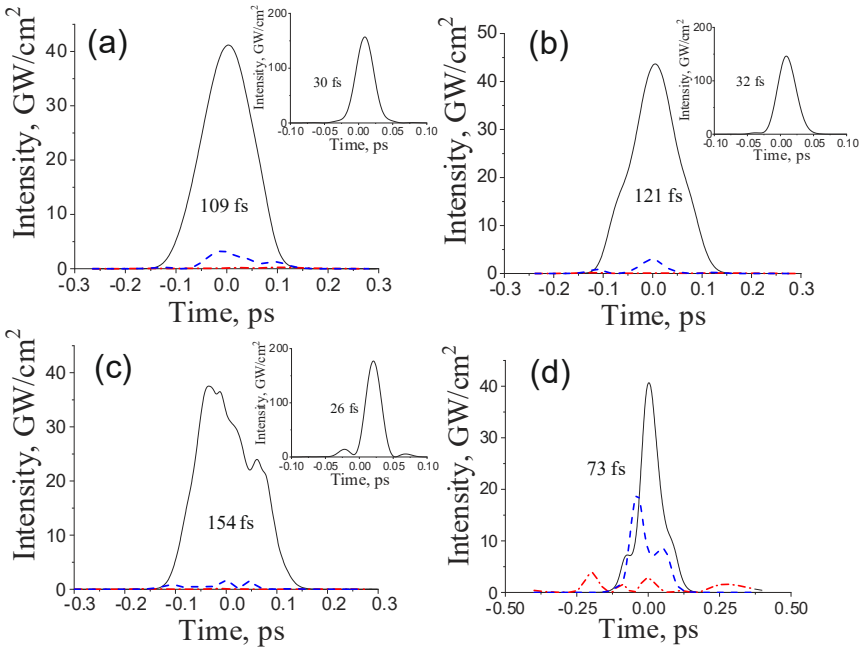

Fig. 6. The profiles of signal (black solid), idler (red dash-dot), pump (blue dash) pulses calculated for propagation distance of 5 mm. (a) profiles for phase modulated input signal with $\gamma = 0$, (b) profiles for phase modulated input signal with $\gamma = 20$, (c) profiles for phase modulated input signal with $\gamma = -20$, (d) profiles when idler absorption is not accounted. Insets show the amplified and compressed pulse envelopes. Pump duration is 100 fs.

simple Gaussian ($A_3 = a_{30}\exp(-r^2/d_{3G}^3)$). The beam width parameters d_{3H} and d_{3G} were chosen to guarantee 1 mm FWHM diameter of pump for both cases. The spatio-temporal profiles of signal and pump wave-packets for hyper-Gaussian pump are depicted in Fig. 7. As can be seen, in lossless case (Fig. 7 bottom line) the signal pulses become modulated and the main part of radiation energy (57%) is contained in pump wave. However, the idler wave absorption makes the situation completely different and leads to formation regular signal pulse (Fig. 7 top line) containing 74% of input energy. The pump pulse acquires the "caldera" type spatio-temporal profile and possess less than 1% of energy. In the case of Gaussian pump beam profile the conversion efficiency to the signal wave drops from 74% to 56%, but is still much better than in lossless case.

All results presented above are obtained for signal wavelength $\lambda_1 = 610$ nm (idler $\lambda_2 = 3.3$ μm), but qualitatively similar results were obtained also for the wavelengths of the signal in range $\lambda_1 = 591 \div 620$ nm (for idler $\lambda_2 = 4.0 \div 3.0$ μm, respectively). The pulse profiles in lossless case presented in Fig. 7 are depicted for the same propagation distances as for the cases with the absorption on the purpose to emphasize that amplification regimes are completely different. We should note, that the signal pulse at the 1-st conversion maximum in lossless case also possess smooth bell-shaped profiles, however the energy conversion is significantly lower and sustains smooth profiles are sustained just for 0.2 - 0.3 mm till pump pulse regeneration starting.

The main drawback of this approach is heating of nonlinear media caused by idler absorption. Nevertheless, the detuning from exact phase matching due to temperature rise can be corrected by adjustment of crystal angle while the crystals fracturing can be avoided by proper crystal cooling or by operating parametric amplifiers at low repetition rate regime.

Optics EXPRESS

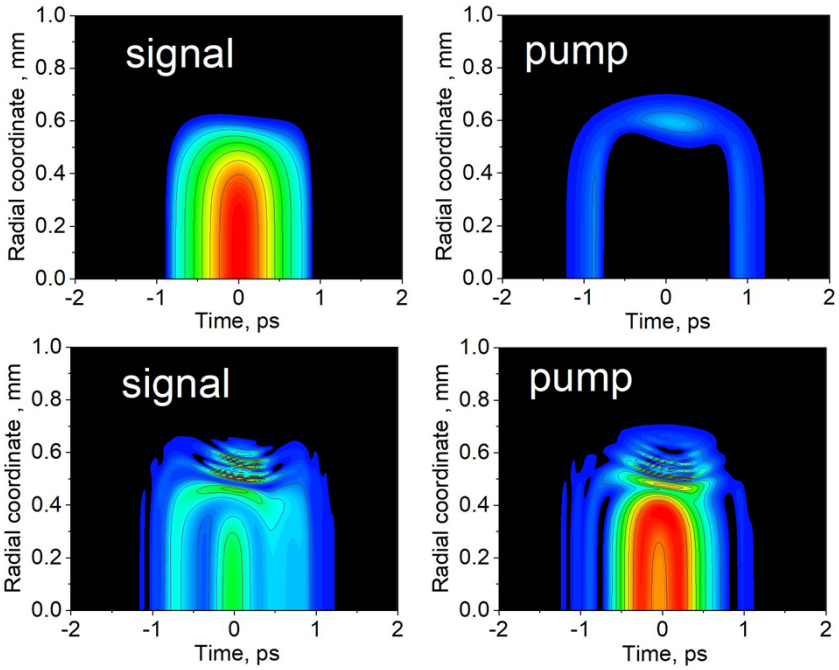

Fig. 7. Signal and pump profiles at the output of 5 mm BBO crystal pumped by 1 mm FWHM hyper-Gaussian beam. Pump pulse duration 1 ps. Profiles in the top row calculated accounting for the idler absorption. In bottom row line results of modeling with switched-off idler absorption.

4. Conclusions

In summary, we have shown that presence of linear absorption for idler pulses can have positive impact on process of parametric amplification. It might increase the spectral amplification band and quench pump regeneration process, thus, leading to signal amplification till nearly total pump depletion. The results of numerical modeling of collinear parametric amplification in 515 nm picosecond and femtosecond pulse pumped type II BBO nonlinear crystal at wavelengths when the idler wave fall into region of strong absorption show that chirped 610 nm signal pulses can be amplified with pump-to-signal energy conversion efficiency of ~75%. In addition, spectral amplification bandwidth can support ~ 30 fs chirped pulses amplification, i.e. can be ~ 2-3 times broader as compared to the lossless case of amplification. The trends obtained in this study can be qualitatively expected for the other nonlinear crystals operated in conditions when one of interacting wave (idler or signal) dissipates energy from interaction zone and we believe that this approach will contribute to future developments of parametric amplification systems.

Funding. Research Projects Implemented by World-class Researcher Groups (01.2.2-LMT-K-718, 01.2.2-LMT-K-718-01-0014).

Disclosures. The authors declare no conflicts of interest.

Data availability. Data underlying the results presented in this paper are available in Ref. [10,11].

References

1. G. Cerullo and S. De Silvestri, "Ultrafast optical parametric amplifiers," Rev. Sci. Instrum. **74**(1), 1–18 (2003).
2. A. Giree, M. Mero, G. Arisholm, M. Vrakking, and F. Furch, "Numerical study of spatiotemporal distortions in noncollinear optical parametric chirped-pulse amplifiers," Opt. Express **25**(4), 3104–3121 (2017)..

Optics EXPRESS

3. D. D. Lowenthal, "CW periodically poled LiNbO3 optical parametric oscillator model with strong idler absorption," IEEE J. Quantum Electron. **34**(8), 1356–1366 (1998).
4. S. C. Lyons, G. L. Oppo, W. J. Firth, and J. R. M. Barr, "Beam-quality studies of nanosecond singly resonant optical parametric oscillators," IEEE J. Quantum Electron. **36**(5), 541–549 (2000).
5. G. Rustad, G. Arisholm, and Ø Farsund, "Effect of idler absorption in pulsed optical parametric oscillators," Opt. Express **19**(3), 2815–2830 (2011)..
6. G. Valiulis and A. Varanavičius, "The broadening of the optical parametric amplification bandwidth caused by idler wave absorption," Lith. J. Phys. **61**(4), 215–221 (2022)..
7. G. Valiulis, "The Influence of Absorption to the Optical Parametric Amplification Bandwidth," in *OSA Nonlinear Optics Conference (NLO)* (2021), paper NTh3A.10, https://doi.org/10.1364/NLO.2021.NTh3A.10.
8. J. Ma, J. Wang, P. Yuan, G. Xie, K. Xiong, Y. Tu, X. Tu, E. Shi, Y. Zheng, and L. Qiani, "Quasi-parametric amplification of chirped pulses based on a Sm^{3+}-doped yttrium calcium oxyborate crystal," Optica **2**(11), 1006–1009 (2015)..
9. Y. Li, H. Zhong, J. Yang, S. Wang, and D. Fan, "Versatile backconversion-inhibited broadband optical parametric amplification based on an idler-separated QPM configuration," Opt. Lett. **42**(14), 2806–2809 (2017)..
10. G. Tamošauskas, G. Beresnevičius, D. Gadonas, and A. Dubietis, "Transmittance and phase matching of BBO crystal in the 3- 5 µm range and its application for the characterization of mid-infrared laser pulses," Opt. Mater. Express **8**(6), 1410–1418 (2018).
11. G. Tamošauskas, "β-Barium Borate (BBO) Absorption in the 0.188-6.22 µm Range," arXiv:2111.01212 (2021).
12. G. Valiulis, A. Dubietis, and A. Piskarskas, "Optical parametric amplification of chirped X pulses," Phys. Rev. A **77**(4), 043824 (2008)..
13. O. E. Martinez, "Achromatic Phase Matching for Second Harmonic Generation of Femtosecond pulses," IEEE J. Quantum. Electron. **25**(12), 2464–2468 (1989).